2023

A simple microcalorimetry system to determine the adsorption behaviour of acids in large adhesive bond gaps using base-initiated solution polymerisation of ethyl-2-cyanoacrylate

Kevin Raheem

John Cassidy

Tony Betts

See next page for additional authors

Authors
Kevin Raheem, John Cassidy, Tony Betts, and Bernard Ryan

A simple microcalorimetry system to determine the adsorption behaviour of acids in large adhesive bond gaps using base-initiated solution polymerisation of ethyl-2-cyanoacrylate

Kevin Raheem [a,b], John Cassidy[a,b], Anthony Betts[a,b] and Bernard Ryan* [c]

[a] *Applied Electrochemistry Group, Technological University Dublin, Camden Row, Dublin, Ireland*

[b] *Chemical and Pharmaceutical Sciences, Technological University Dublin, Grangegorman, Dublin, Ireland*

[c] *Henkel Ireland Ltd, RD&E, Tallaght Business Park, Whitestown Industrial Estate, Dublin, Ireland*

Abstract

This work presents the use of a simple microcalorimetry cyanoacrylate (CA) polymerisation system for investigating aspects of CA adhesive cure through gap and adsorption of adhesive acid stabiliser by a range of metal and glass substrates. It is well established that strong acid induced inhibition periods (IPs) are almost directly proportional to the acid concentration in weak base initiated polymerisations of alkyl CAs in tetrahydrofuran (THF). Ethyl cyanoacrylate (ECA) polymerisation IP measurements were used to determine the adsorption of methanesulfonic acid (MSA) in THF or ECA solutions by a range of metal, glass and polypropylene (PP) lap shears surfaces. The extent of substrate acid sorption was found to decrease in the order: Copper- zinc alloy (C23000) > grit blasted mild steel > aluminium alloy 2024T3 > mild steel > glass > aluminium > stainless steel alloy 304 > PP. Differences in the extent of acid sorption were accounted for in terms of two effects: surface acidity/basicity and surface area (roughness). The decrease in MSA concentration following lap shear immersion in an MSA solution was related to the reactivity of the substrates for catalysing bond line polymerisations as described in a recently reported confocal Raman spectroscopic study of ECA /substrate reactivity.

Key Words: cyanoacrylate, metals, lap-shear, acid-base interactions, microcalorimetry

1. Introduction

The kinetics of anionic/ zwitterionic CA dilute solution polymerisations have been extensively investigated by Pepper et al [1-5]. Composite initiation, propagation and termination rate constants were determined in a range of solvents using both neutral bases and anion initiators [6-9]. Bykova and co-workers used adiabatic and isothermal calorimetry to study the thermodynamic properties of CA polymers [10]. The concentrations of strong and weak acids present in CA adhesives were investigated by Stefanov et al using calorimetric techniques [11].

The cure performance and mechanical strengths of CA adhesives is influenced by the chemical and physical nature of the adhesive/substrate interface. In many cases little is known about the interfacial interactions. CA adhesives are readily cured by surface nucleophiles in nominally zero gap (2-10 µm) bonds. However, overall cure speed rapidly decreases with increasing bond gap which limits the applicability of CA adhesives. The decrease in overall cure speed with increasing bond gap can at least partly be attributed to the presence of strong acid stabiliser in the adhesive which neutralises surface base and inhibits the anionic/zwitterionic polymerisation. In a related study to that presently described, the kinetics of CA depth curing through 100 µm bond gaps on a range of metal substrates was investigated using Confocal Raman Microscopy[12]. Polymerization rates were

**Corresponding author: E-mail address: rben1591@gmail.com*
Abbreviations: IP - inhibition period, ECA - ethyl-2-cyanoacrylate, MSA - methanesulfonic acid GBMS - grit blasted mild steel, AL - aluminium, PP - polypropylene

highly dependent on substrate type and progressively decreased with increasing distance from the substrate surface. The main objective of this initial study was to gain a better understanding of bond line adhesive acid reactions during gap curing. The adsorption of a strong acid stabiliser (MSA) from both THF and ECA monomer by a range of substrates was investigated. The substrate surface area to THF or ECA volume ratio was similar to that of a 100 µm bond gap. Apart from mimicking bond line gap condition, the large area to volume ratio greatly enhanced the sensitivity of the acid measurements.

The importance of acid/base properties in heterogeneous solid catalysis is well documented and has been extensively studied for a wide range of catalysed reactions [13, 14]. These properties can be investigated by studying the adsorption of suitable probe molecules on the substrate using physicochemical methods such as NMR spectroscopy [15], potentiometric titration [16, 17] and calorimetry [18-21]. The most utilised method for monitoring the presence of surface hydroxyl species is Infrared Spectroscopy through the measurement of frequency shifts or change in relative intensities of absorption bands arising from the protonated and coordinated forms of probe molecules [22-24]. Silbaugh investigated the Brønsted acidities on anatase TiO_2 using FTIR by measuring the shift of sensitive bands of the various alcohol probe molecules [25]. Busca systematically explored different qualitative FT- IR techniques for evaluating oxides including the use of polymerisation based indicators such as 1,3-butadiene liquid adsorbed onto aluminium oxide (Al_2O_3) [26]. Thermochemical techniques such as differential thermal analysis or differential scanning calorimetry have been used to investigate the acid/base character of solid surfaces. Adsorption is generally exothermic, therefore when a probe molecule adsorbs onto a solid surface, the heat evolution can be measured. This heat is related to the ability of the surface sites to interact with the probe molecule indicating the basic or acidic character [19].

The abovementioned methods of adsorption analysis have their advantages and disadvantages. Typically, they are time consuming and require use of sophisticated equipment and sample preparation techniques that cannot readily be used to investigate adhesive substrate interactions. CA adhesives are usually acid stabilised. Reactivity depends on a carefully formulated balance between stabilising acid content and acceptable product shelf life. Initiation by surface nucleophiles, including water, that result in anionic/zwitterionic polymerisation is the commonly accepted explanation for bond line curing. Surface adsorption of stabilising acid could greatly increase adhesive reactivity and play an important role in curing on many substrates. The main objective of this work was to investigate the extent of acid adsorption from both THF and ECA solutions by a range of substrates. Reaction of acid with soluble surface base, and ECA polymerisation by soluble base/nucleophile was also investigated. The work is exploratory in nature and used higher acid concentrations than normally employed in stabilised CA adhesives.

2. Materials and Methods

2.1 Materials

The chemicals used in this study were all analytical purity obtained from Sigma Aldrich Ltd (Ireland) and VWR. The THF was HPLC grade and was used without further purification. ECA that was stabilized with ppm quantities of strong acid and non-stabilised distilled ECA were used for the experiments. Both monomers were supplied by Henkel Ireland Ltd. and were stored at 2-4 ^{0}C. Standard Q-Lab test lap shears (1.5 x 25 x 100mm) shears were cleaned by twice wiping with isopropyl alcohol soaked lint free paper prior to use. Table 1 shows the composition of the seven

substrates that were studied. Polypropylene (PP) was used as a non-reactive control substrate. The glass substrate was a 1.0 x 26 x 76 mm soda lime glass microscope slide. No corrections were made for the consequent decrease in the slide surface area/solution volume ratio.

Table 1: *Substrate composition (% w/w) from supplier's specifications and surface roughness*

	Aluminium	**Aluminium 2024T3**	**Mild Steel**	**Grit Blasted Mild Steel**	**Stainless Steel (304)**	**Copper Alloy C23000**	**Soda Lime Glass**
Aluminium	99.3	90.7-93.1	-	-	-	-	4.2
Boron	-	-	-	-	-	-	8.4
Carbon	-	-	0.15	0.15	0.08	-	-
Chromium	-	0.1	-	-	18 - 20	-	-
Copper	0.10	3.8-4.9	-	-		84 - 86	-
Iron	-	0.5	99.2	99.2	66.5 - 71.1	0.05	-
Manganese	0.05	0.3-0.9	0.60	0.60	2	-	-
Magnesium	0.05	1.2-1.8	-	-	--	-	-
Nickel	-	-	-	-	8.00 10.50	-	-
Potassium	-	-	-	-	-	-	6.9
Silicon	-	0.5	-	-	0.75	-	64.1
Sodium	-	-	-	-	-	-	6.4
Titanium	0.03	0.15	-	-	-	-	4.0
Zinc	0.10	0.25	-	-	-	15	5.9
Others (total)	0.03	0.15	0.065	0.065	0.1	0.05	0.1
Surface Roughness Ra (nm)	<200	<200	1000	1550	<200	1300	3

2.2 Microcalorimeter

A schematic diagram of the calorimetry measuring apparatus is shown in Figure 1. The calorimeter consisted of a PP reaction vessel insulated by an air gap provided by a glass outer wall. Heat loss was significant due to the calorimeter's large surface area to volume ratio. Exotherms were measured using a bare junction type K thermocouple (TC) that partially penetrated, without perforation, the base of the PP container. Use of an external TC had the advantage of simplicity however, the insulating effect of the PP base imposed a time delay of approximately 4s in the detection of an exotherm onset. Allowing for the time delay, IPs could be accurately determined. Owing to variable rates of heat lose and thermocouple positioning, post IP polymerisation rates could only be very approximately determined, and unlike the IP measurements, had poor reproducibility in replicate experiments. An example of this behaviour is shown in Figure 9. Thermograms were recorded using a Visual BASIC program and a Pico Technology TC-08 USB data logger and displayed in real time on a Windows PC. All experiments were conducted at room temperatures, typically between 18-22°C, at 30%-40%RH. Replicate experiments were carried out in all cases to evaluate IP reproducibility. The thermogram of a typical MSA inhibited ECA polymerisation in THF is shown in Figure 2.

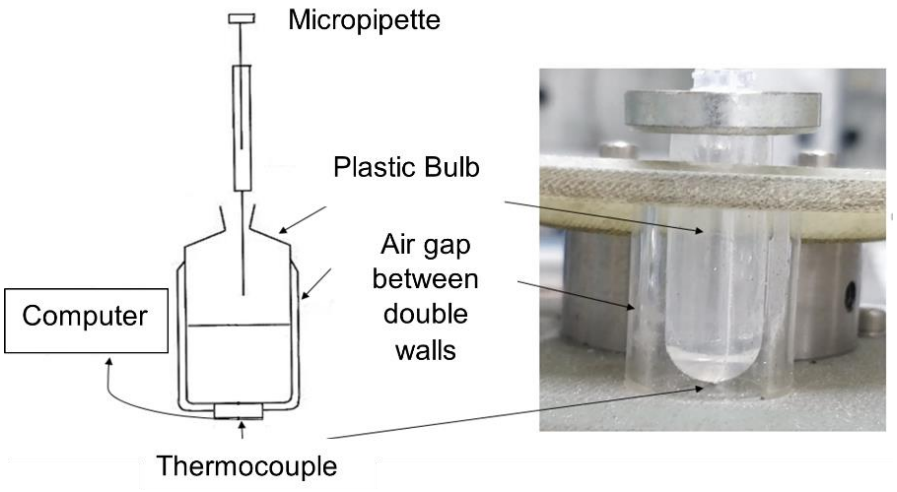

Figure 1: *Micro calorimeter that contains 172 µL of ECA/THF reaction mixture.*

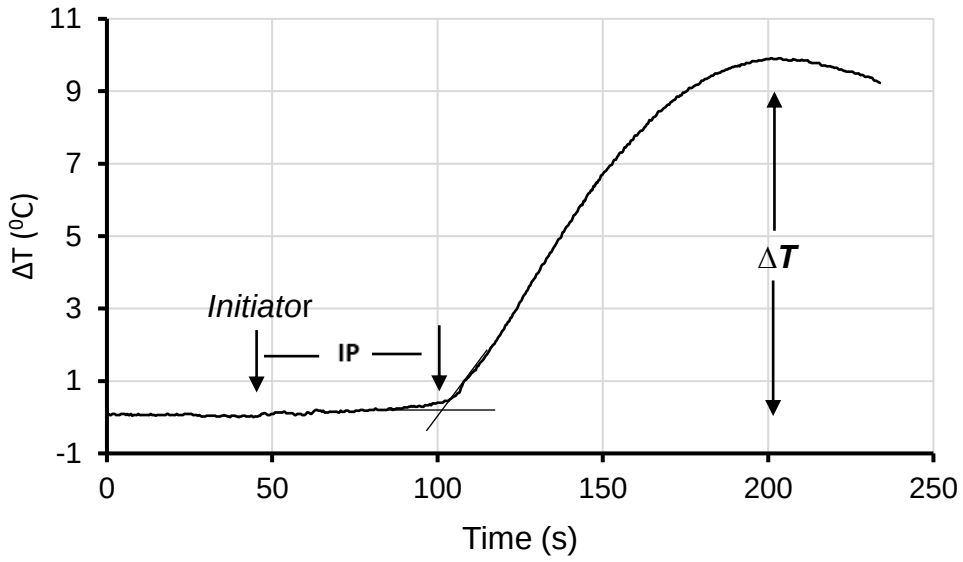

Figure 2: *Thermogram of an MSA inhibited, polymerisation of 50% v/v ECA/THF solution. The inhibition period (IP) is the time difference between the initiator injection and the intersection point.*

2.3 Adsorption Jig - Equivalence to 100 µm Bond Gap

The adsorption jig was fabricated from PTFE. It comprised of a precision cut chamber that allowed a small volume (180 µL) of an MSA solution in ECA or THF to wet a large area of an inserted lap shear. The lap shear volume to surface area ratio (5.25 ul/ cm^2) approximated that of a 100 µm adhesive bond gap to identical adherends. The small volume to surface area ratio also much enhanced the

sensitivity of the acid sorption measurements. Reagent concentrations were optimised to maximise reproducibility and substrate selectivity.

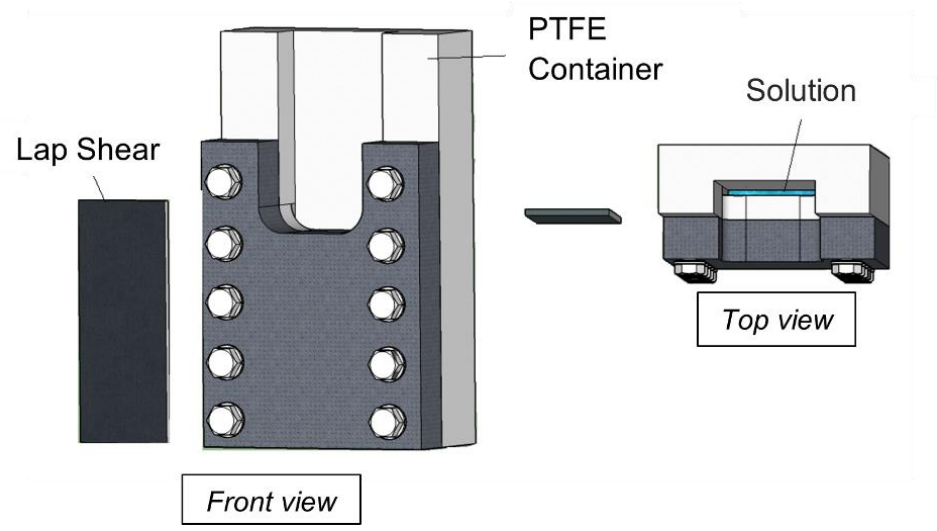

Figure 3: *Schematic of the jig apparatus used for the MSA adsorption experiments.*
An aliquot was removed from the jig MSA solution and added to the calorimeter immediately after the allocated adsorption/reaction time to minimise solvent evaporation.

2.4 Experimental Method

As mentioned above, THF and ECA monomer were used as solvents for the acid adsorption studies. Surface basicity/adsorption was investigated by immersing a lap shear in 180 µL of acidified solvent in the PTFE jig (Figure 3). After a set reaction time (180s), an aliquot (86 µL) of MSA/THF solution was added to 86 µL ECA in the calorimeter. The procedure was reversed for adsorption from ECA. The mixture was polymerised with 43 µL of either a 0.2% or 1% w/v solution of 3,5-dichloropyridine (DCP) in THF, denoted as solution A and B respectively, and the resultant IP was measured. The decrease in IP following lap shear immersion was compared with an IP vs MSA calibration and gave a measure of the quantity of MSA that was consumed in surface reactions. IPs occur following the addition of many types of slowly initiating weakly basic species to acidified CA monomer solutions. DCP was used because of concentration considerations and its long-term stability in THF.

Prior to initiator injection, the temperature of the reaction mixture was sampled for 45s to ensure pre-polymerisation was not occurring and a stable temperature was maintained c.f. Figure 2. The IP was taken as the time interval between initiator injection and the intersection of linear projections from the acid inhibited and initial rapid phase of the thermogram as shown in Figure 2. Because of the gradual transition from inhibition to rapid polymerisation, the measurement method only gives an approximation of the MSA concentration. However, errors are not significant as uncertainty in determining the “end of” an IP are small compared to the overall IP length. Plots of IP versus MSA concentration were linear (c.f. Figures 6 and 8). Thermogram analysis using an R Studio piecewise segmented regression methodology [31-33] yielded similar IPs to the intersection method described above. Before each experiment, the jig was exhaustively washed with THF and allowed to air dry.

3. Strong Acid Calibrations

3.1 0-10 ppm MSA/THF

The system was calibrated by adding 86 µL of MSA/THF calibrant solutions to 86 µL of distilled ECA monomer in the calorimeter PP bulb. Polymerisations were initiated by the addition of 43 µL of initiator in THF (solution A). The corresponding thermograms are shown in Figure 4. Negligible differences in the pre and initial post initiator injection thermogram slope were usually recorded.

A plot of IP versus acid concentration was linear, with a slope of 5.3 s/ppm and a non-zero y-intercept of 6.2s, c.f. Figure 5. Allowing for the time delay imposed by slow heat transfer to the thermocouple mentioned earlier, this indicated a strong acid concentration in the distilled monomer of 1.2 ppm expressed as equivalents of MSA. The proportionality between IP and acid concentration in related systems was previously reported [7].

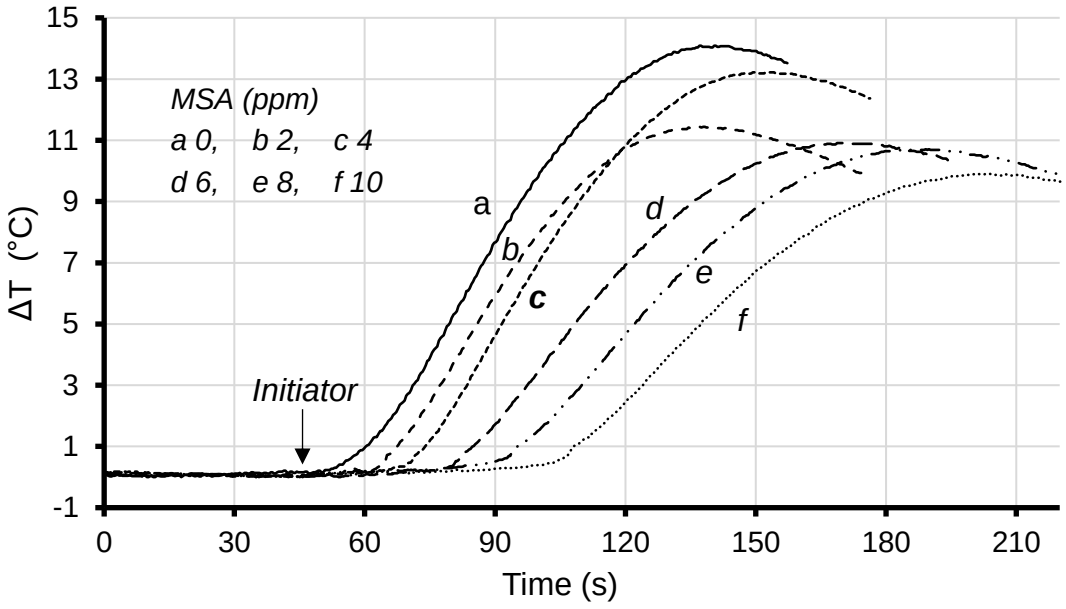

Figure 4: *MSA (0-10 ppm) IP calibration thermograms using distilled ECA.*
86 µL MSA/THF calibrant solutions directly added to 86 µL of distilled ECA. Initiated with 43 µL of solution A.

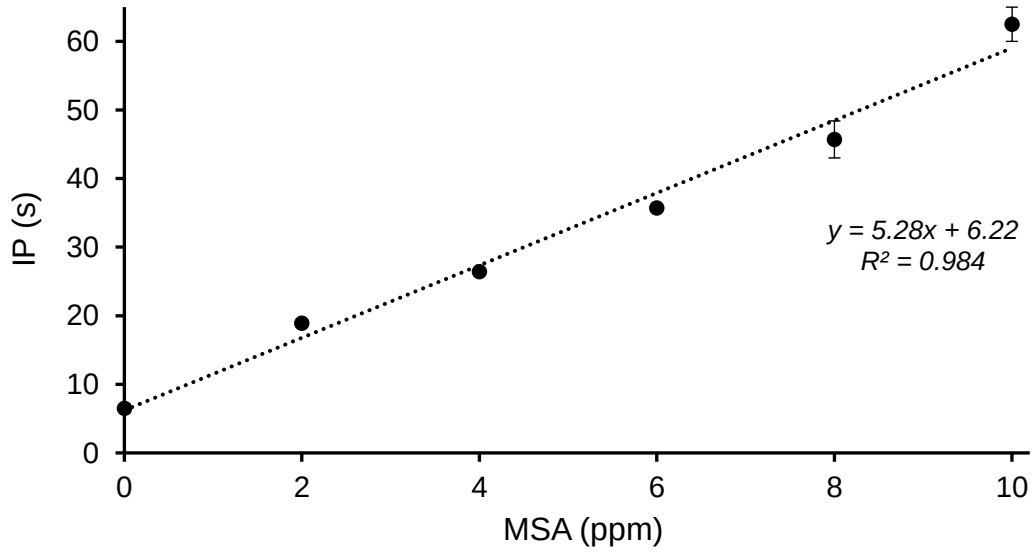

Figure 5: *Plot showing the linear relationship of the thermogram inhibition periods in Figure 4 versus MSA concentration. The data points were averaged from two replicate experiments.*

3.2 0-200 ppm MSA/THF

Figures 6 and 7 show the post initiator injection thermograms and corresponding calibration plot obtained over a larger MSA (0-200 ppm) concentration range. Acid stabilised ECA monomer was used in this case owing to limited availability of distilled monomer. A fivefold higher initiator concentration (solution B) was also used.

In contrast to the 200 ppm MSA IPs, the 0-100 ppm IPs had good reproducible in replicate experiments (c.f. calibration plot error bars Figure 7). The 200 ppm MSA data point was omitted from the calibration as there was large IP variations in replicate polymerisations (193-224 s) which were also considerably less than that a projected IP of 292 s. The large variations, that requires further investigation, may indicate solubility issues with the initiator/MSA salt that forms following addition of initiator to the calorimeter. The 224 s IP exotherm is included in Figure 6.

The MSA adsorptions of the more strongly MSA adsorbing substrates summarised in Figure 10 are based on the 0-100 ppm MSA calibration. The results for the less adsorbing PP, steel 304 and aluminium substrates were based on a linear calibration that included all the MSA data points.

The inhibiting acid concentrations in the distilled and stabilised ECA, expressed as MSA equivalents were 1.2 and 3.2 ppm respectively. The values were calculated from the corresponding y-intercepts in Figures 5 and 7.

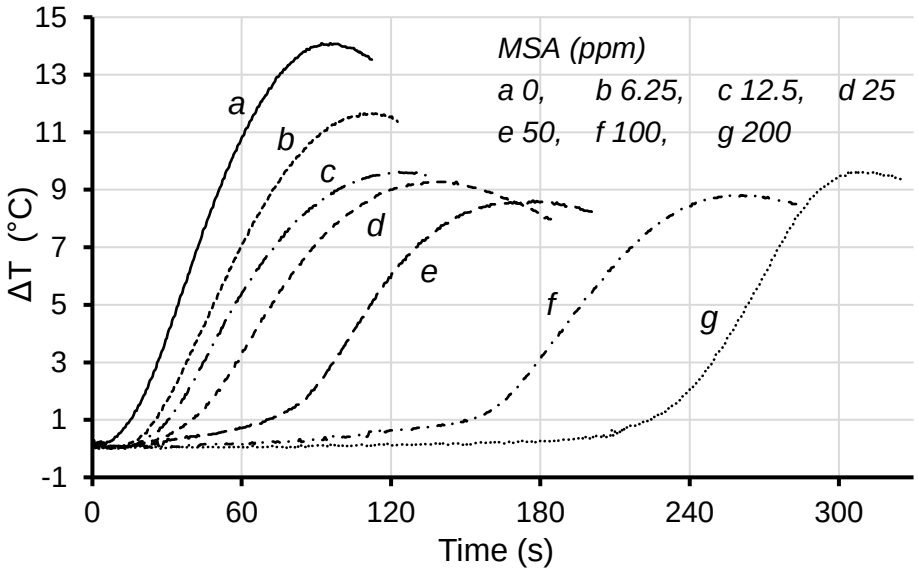

Figure 6: *MSA (0-200 ppm) IP calibration thermograms using stabilised ECA - Post initiator injection 86 µL MSA/THF calibrant solutions directly added to 86 µL of acid stabilised ECA. Initiated with 43 µL of solution B. Only the post initiator injection thermograms are shown.*

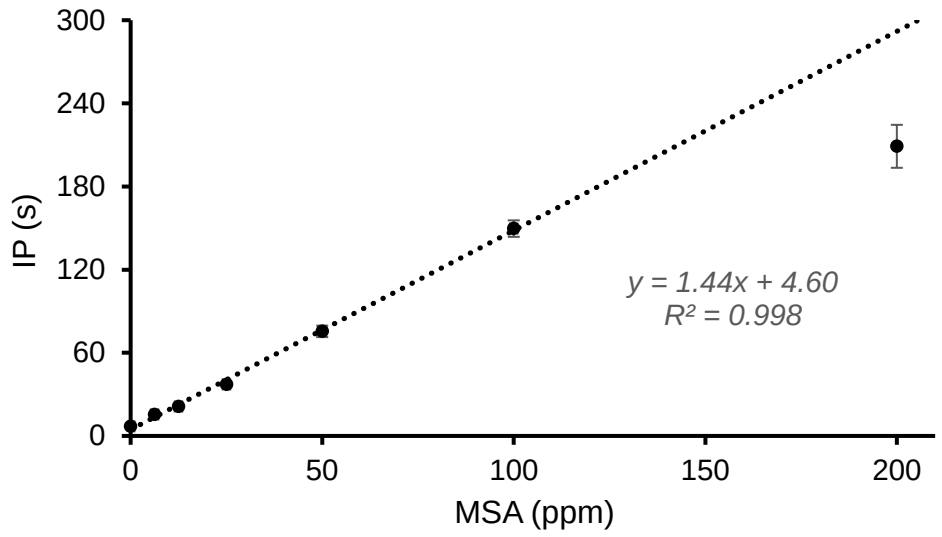

Figure 7: *Plot of the inhibition periods in Figure 6 versus MSA concentration. The data points were averaged from two replicate experiments. The 200 ppm data point was not included in the regression plot.*

4. Results and Discussion

4.1 MSA/THF Adsorption - Polypropylene

A PP lap shear of nominally identical dimensions to that of the metal test specimens was used as a control to check for the presence of acidic or basic impurities in the jig prior to use of the system. On a non-polar, low surface energy substrate such as PP, no significant MSA adsorption should occur. The PP lap shear was placed in the adsorption jig containing a 10 ppm MSA/THF solution for 180s. The resulting jig solution thermograms were almost superimposable with the thermograms that were obtained from direct addition of the MSA solution to the calorimeter c.f. Figure 8. The slightly shorter IP of the PP jig solution corresponds to an MSA concentration of 9.5 ppm and indicates that that MSA adsorption by the PP lap shear and jig and was insignificant. No significant IP differences were observed when the PP jig solution adsorption time was varied from 30 to 180s.

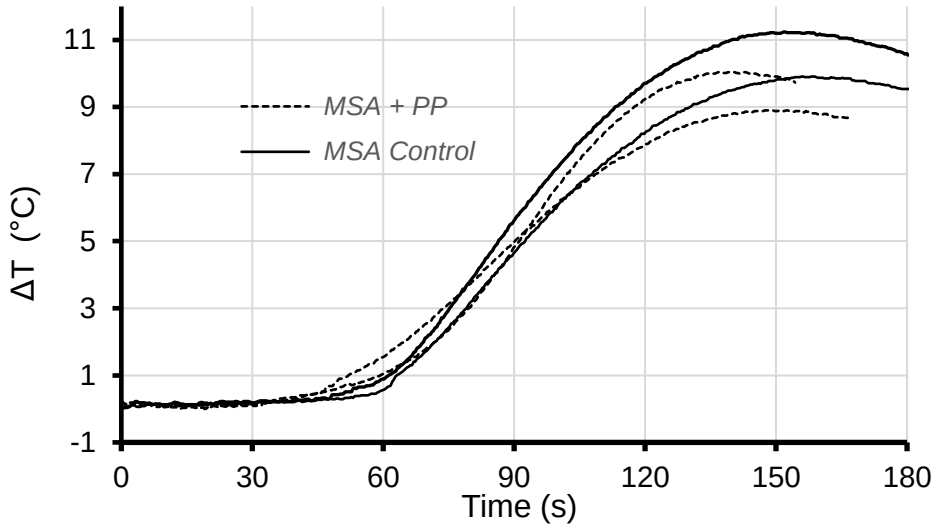

Figure 8: *Effect of PP lap shear of 10 ppm MSA/THF adsorption on resulting IPs.*
86 µL of MSA/THF solution was removed from the jig after 180s and added to 86 µL of non-stabilised ECA in the calorimeter. "MSA Control" refers to substitution of the jig MSA/THF with 86 µL of directly added 10 ppm MSA/THF to the calorimeter. The polymerisations were Initiated with 43 µL of solution A. Post initiator injection replicate polymerisations.

4.2 MSA/THF Adsorption - Metal and Glass

A 200 ppm MSA THF solution was used in preference to a 10 ppm solution for the substrate adsorption experiments as it was found that the former solution provided large substrate dependent IP differences c.f. Figure 9. Similar substrate dependent IPs were observed in a related study mentioned earlier that used Confocal Raman Microscopy to investigate curing of acid stabilised bulk ECA adhesive in 100 µm bond gaps[12].

The extent of MSA adsorption by the various substrates is compared in Figure 10. (For display clarity the Glass and Copper replicate exotherms were omitted in Figure 9.) It is presumed that the strong acid was mostly removed by reaction with surface species such as oxides, hydroxides, and carbonates although reaction of MSA with base metal was also possible. GBMS and copper alloy lap shears exhibited the shortest IPs and removed 115 and 123 ppm of MSA respectively from the 180 ppm MSA jig solutions. As expected, the larger surface area of the GBMS lap shear compared to its non-grit blasted counterpart resulted in 1.7 fold increased MSA sorption.

The IP measurements may provide an estimate of surface oxide reaction depths. For example, the MSA adsorptions of the AL and AL2024 lap shears were approximately 1.0 and 4.9 nmol cm^{-2} respectively (c.f. Figure 10). Omitting the contribution of other surface species, this corresponds to reaction depths in terms of aluminium oxide of 0.043 and 0.21 nm (using the oxide bulk density of 3.97 g cm^{-3} and quantitative conversion of oxide to tri mesylate salt). The respective depth values are only a small fraction of reported aluminium oxide surface layer thicknesses. The higher reactivity of AL2024 may be related to its relatively high magnesium content (c.f. table 1). However, interpretation of the results is speculative owing to the limited experimental data. Similar low fractional reaction depths were calculated for the other metal substrates even using stoichiometric MSA/surface oxide ratios as small as 1:1. The results are further complicated by the possibly that the reaction depths are underestimated owing to possible effects of metal mesylate salts on the IPs.

Reaction rate measurements, use of variable initial MSA concentrations, and measurement of post reaction jig THF metal ion content should reveal more detailed information regarding the reactivity of surface species. Further aspects of surface reactivity are discussed below.

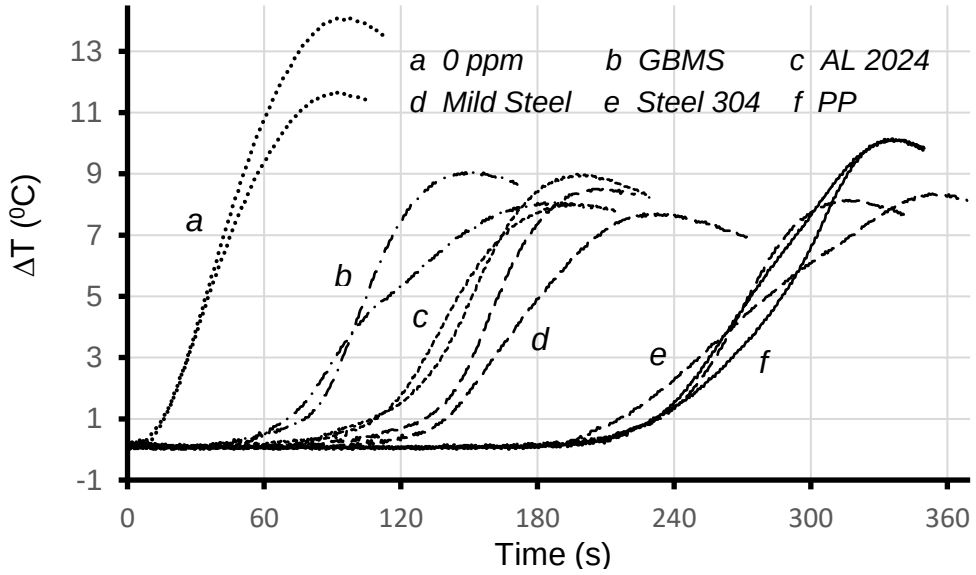

Figure 9: *MSA/THF – Replicate polymerisations showing the effect of various lap shears on resulting IPs.*
180 µL of 200 ppm MSA/THF jig solution
86 µL of the solution was removed from the jig after 180s and added to 86 µL of stabilised ECA in the calorimeter. The 0 ppm label refers to substitution of the jig THF with 86 µL of directly added non acidified THF. The polymerisations were initiated with 43 µL of solution B. - post initiator injection replicate polymerisations.

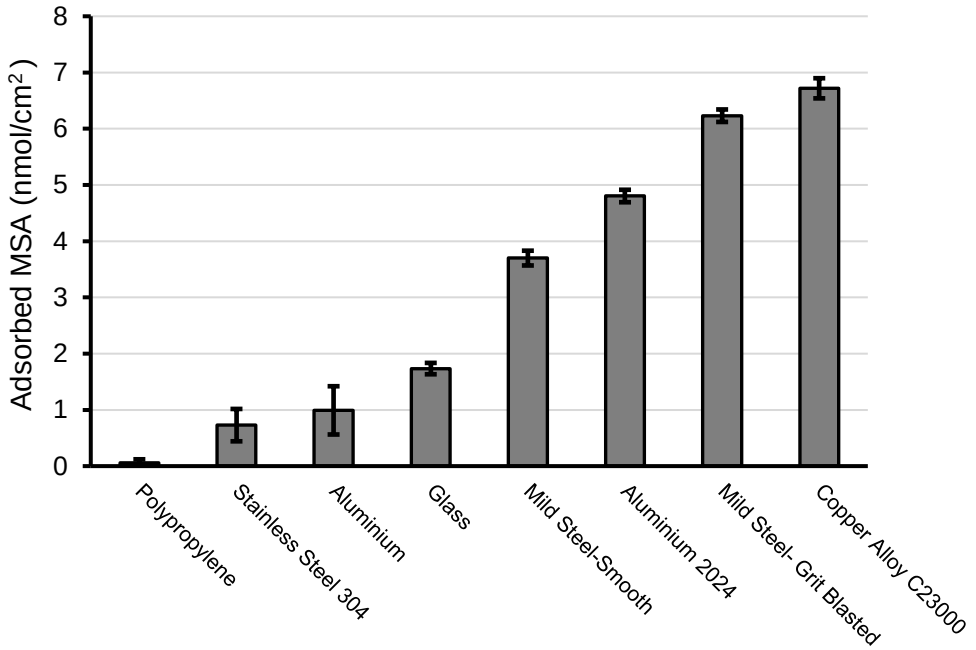

Figure 10: *Substrate MSA adsorption (nmol cm^{-2}) from a 200 ppm MSA/THF jig solution. The corresponding calorimeter exotherms are shown in Figure 9. c.f. section 3.2 also. The copper alloy column represents 61% MSA adsorption.*

Apart from the depth and morphology of reactive surface species, humidity dependent differences in the rate of MSA adsorption could also affect the IP results. Adsorbed water layers are present on most metal surfaces through formation of hydrogen bonds on top of already formed hydroxyls, as illustrated in Figure 11 [27, 28].

On a micro scale, different rates and extents of acid adsorption take place [27]. Several types of sites may coexist on the surface at the same time [29]. Studies of adsorbed water on aluminium oxide surfaces have shown that surface coverage is not uniform and there are surface regions where no water molecules are present even under high humidity conditions [30].

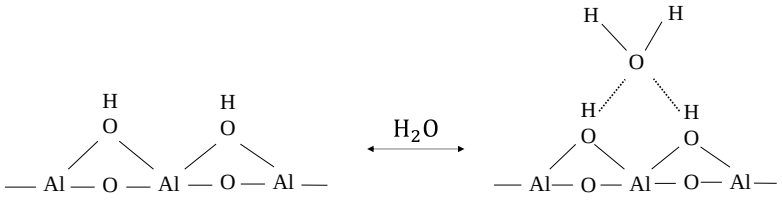

Figure 11: *Illustration of secondary water layer formation on hydrated aluminium oxide surface under ambient conditions. The reactivity and complexity of the surface structure are affected by humidity and ageing.*

Aluminium oxides/ hydroxides exist in several forms with varying crystalline structures and stabilities [36]. As shown in Figure 10, the 100% AL surface lap shear interacted less strongly with MSA compared to its alloy counterpart AL2024 that contained trace amounts of Cu, Mg and Mn [37]. The presence of divalent oxides such as MgO may lead to sites of higher basicity that could reduce the overall acidity of the aluminium alloy surface compared to the pure aluminium surface [38]. McCafferty showed that adsorption of the chloride anion onto the oxide layer of an aluminium surface is favoured compared to its adsorption on a tantalum oxide implanted aluminium alloy surface. This is because the oxide layer of a pure aluminium oxide surface contains primarily acidic surface groups [39]. Similarly, in the case of stainless steel, high amounts of chromium oxide Cr_2O_3 may increase the acidity of the 304 steel surface compared to the more reactive mild steel [40]. Auroux et al reported similar low adsorption characteristics of Cr_2O_3 by measuring the differential heats of adsorption of the Lewis base NH_3 [19]. This supports the notion that the presence of chromium oxide may increase the surface acidity of an alloy metal.

The metal and silicate surfaces that were tested in this study are known to have similar hydrated surface oxide layers. Like metal alloy oxides, Si–O bonds can react with water to form hydroxyl groups. Ion-exchange between H^+ and network modifying cations held in the soda lime glass matrix e.g. Na^+ and Ca^{2+} could also occur [34, 35]. Despite its basic nature, the glass removed significantly less inhibiting species from the THF than most of the other substrates that were tested.

A study of the effect of varying reaction time, humidity, temperature and acid concentration on resultant IPs may provide a more detailed picture of surface composition and reactivity. Such considerations were beyond the scope of this initial investigation. Unlike strong acid, weak acid

adsorption rates should be more sensitive to surface species type. Initial experiments are described in a following section.

4.3 MSA/ECA Adsorption - Polypropylene and Metals

In reversal of the procedure described in the earlier sections, MSA/ECA solutions were substituted for MSA/THF in the adsorption experiments. In order to check the methodology, the effect of directly adding 86 ul 10 ppm MSA/ECA (distilled) to 86 ul pure THF was compared with that of adding 86 ul 10 ppm MSA/THF to 86 ul of distilled ECA. Both solutions were initiated with 43 µL of solution A. Resulting IPs were closely similar c.f. Figure 12.

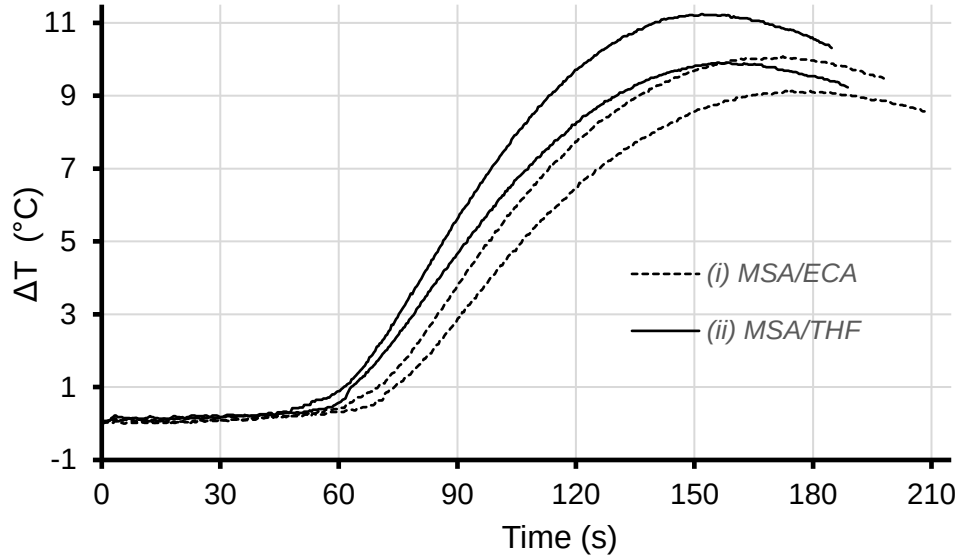

Figure 12: *Comparison of direct addition to the calorimeter of:*
(i) 86 µL 10 ppm MSA/ECA (distilled) added to 86 µL non acidified THF
(ii) 86 µL 10 ppm MSA/THF added to 86 µL ECA (distilled)
Polymerisations initiated with 43 µL of solution A - post initiator injection replicate polymerisations.

Owing to potential contamination problems associated with formation of poly ECA in the jig, only a limited number of MSA/ECA adsorption experiments were carried out. The extent of MSA adsorption on PP, AL2024 and Steel 304 substrates was investigated using 100 ppm MSA/ECA solutions. As expected, the PP and directly added 100 ppm/ECA IPs were almost identical (~115s) c.f. Figure 13. The relative difference in the PP, AL2024 and Steel 304 MSA/ECA IPs were similar to those of the corresponding MSA/THF IPs c.f. Figures 13 and 9 respectively, indicating at least for these substrates, that the extents of MSA adsorption from THF and ECA was similar. Apparently, possible very rapid surface ECA polymerisation did not prevent significant acid adsorption. It is important to note that the MSA concentration in the abovementioned experiments was much higher than normally employed in ECA adhesives. The results, therefore, do not rule out the possibility that rapid surface polymerisation of low acid content adhesive could impede surface adsorption/dissolution processes.

The results demonstrate that substrate acid adsorption may be an important parameter in ECA adhesive bonding. The extent of MSA adsorption from stabilised ECA by various substrates could be quantified by a calibration similar to that described for the MSA/THF solutions.

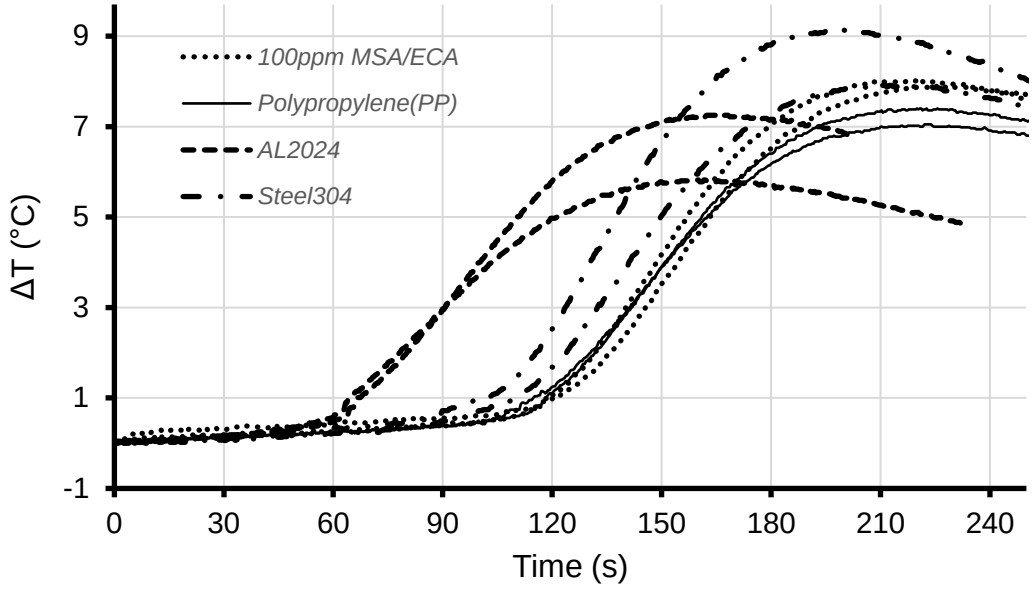

Figure 13: *100 ppm MSA/ECA - Effect of PP, steel and AL2024 lap shears on resulting IPs. 180 µL of 100 ppm MSA/ECA jig solution, 86 µL of the solution was removed from the jig after 180s and added to 86 µL of non-acidified THF in the calorimeter. 100 ppm label refers to 100 ppm MSA/ECA directly added to the calorimeter. All polymerisations Initiated with 43 µL of solution B. - post initiator injection replicate polymerisations.*

4.3 Weak Acid Adsorption

Apart from initiation by surface base, initiation by adsorbed surface water is also thought to play an important role in CA bonding. Water also affects the activity of Brønsted acid or base sites. For example, Fang et al demonstrated that increased %RH reduced the amount of weak acid adsorbed on silica particle surfaces which implied adsorption of water vapour may inhibit surface reactivity by blocking adsorption sites and promote dissociation of H_3O^+ ions and anions [41]. This competition mechanism has been suggested by others [42]. Brønsted sites can also be distinguished from Lewis sites by choice of probe molecule. Chemisorption experiments using weak Brønsted and Lewis acids of varying strength may provide more detailed information regarding surface species. Initial results using a thermistor-based system [11] that measured rate retardations in dilute solution ECA/THF polymerisations have shown that, similarly to MSA, adsorption of cyanoacetic acid from a 400 ppm solution in THF was highly substrate dependent. A combination of microcalorimetry and spectroscopic techniques such as Raman [12] or FT-IR could provide a more detailed picture of the interactions of acidic species during CA bond line curing.

5. Soluble Base Released from a Substrate Surface

5.1 Reaction with MSA

The preceding sections have shown that immersion of glass and a range of metal lap shears in a small volume of either MSA/ECA or MSA/THF resulted in significant decreases in the inhibiting species concentrations of both solvents. Apart from MSA surface interactions, it was also possible that MSA neutralisation by soluble surface base could have contributed to the decreased acid

concentration. In order to test this hypothesis, PP, glass, and GBAL lap shears were immersed in 180 µL of non-acidified jig THF and gently agitated for 20 minutes using a laboratory shaker. 86 µL of the jig solvents were subsequently added to the calorimeter that contained 86 µL of acid stabilised ECA and 86 µL 10 ppm MSA/THF and polymerised with 43 µL of solution A. Within experimental uncertainty, all the resulting thermograms were closely similar and matched those of control thermograms that were obtained using non jig treated pure THF.

The above results indicate, at least in the case of glass and GBAL, that surface interactions were almost entirely responsible for removal of MSA from acidified THF. Use of lower acid concentrations and larger surface area to volume ratios would provide a more sensitive measure of the extent of surface base solubilisation and acid adsorption in a CA adhesive bond line.

5.2 Initiation of Polymerisation

As discussed above, high acid concentrations may have swamped effects of soluble surface base on decreasing the IPs. The results therefore do not exclude the possibility that, even in the absence of significant acid adsorption by bond line substrates, adhesive soluble surface base could cause rapid bond line polymerisation. This could particularly apply to nominally zero gap bonds that have very large surface area to adhesive volume ratios.

In order to investigate this possibility, the acid concentration in the system was minimised by reducing the quantity of acid stabilised ECA from 80 to 3 µL. The smaller resultant exotherms necessitated use of a highly temperature sensitive thermistor probe that was directly inserted into a 3 µL ECA solution in 100 µL acid free THF in a 1 ml calorimeter. The calorimeter was of similar design to the larger scale version reported by Stefanov et al [11]. Preliminary results have shown that initially rapid polymerisations were initiated, following addition to the rapidly stirred ECA calorimeter solution, of 100 µL of acid free jig THF that was in contact with glass, GBAL and GBMS lap shears for 180s. However, no measurable polymerisation occurred using PP and non-grit blasted AL2024 lap shears. These results indicate, at least for the former set of substrates, that there was sufficient THF soluble surface base or nucleophiles to initiate polymerisation of the small volume of acid stabilised ECA. It is important to note that the solvating power of THF for surface species may be significantly different to that of ECA. In this context, solvents with similar solvating properties to ECA such as ethyl cyanoacetate could be used instead of THF for the adsorption experiments. The THF results do, however, indicate that significant quantities of ECA soluble nucleophilic species are available on many surfaces.

As discussed in a previous section, surface water is also thought to be an effective initiator of ECA bond line polymerisations. Water present in the adhesive could also enhance adhesive solubilisation of surface species. The water content of the HPLC grade THF (<0.1% specification) was not determined. On the time scale of the experiments it did not destabilise the ECA solutions. This was in accordance with the findings of a previous report that showed a much higher water content was required to cause polymerisation of ECA in THF [43]. Unlike most anionic polymerisations that are rapidly terminated by water, the anionic/zwitterionic propagation rate in pyridine initiated polymerizations in THF was found to be largely unaffected by low water concentrations. The insensitivity was attributed to the extreme reactivity of the monomer. A further finding was that 1.0% water almost doubled the pyridine ECA initiation rate [43]. The most important effect of water

on the adsorption IPs may have been to increase the THF solubility of potentially inhibiting metal mesylate salts. Use of lower acid concentrations may reveal whether adhesive water content significantly increases solubilisation of surface nucleophiles.

6. Conclusions

The adsorption of MSA from both THF and ECA solutions by PP, soda lime glass and a range of metal substrates was investigated using simple micro calorimetric techniques. There was a wide variation in the extent of acid adsorption by the various substrates that may reflect the quantity and reactivity of basic surface species. Stainless steel 304 and a copper zinc alloy had the respective lowest and highest reactivities. Interpretation of the results was complicated by the possibility of interference by metal mesylate salt reaction products. MSA adsorption was determined at only one acid concentration and adsorption time. Investigation of adsorption kinetics and soluble mesylate salt content is required for a more complete characterisation of the reactivity and concentration of surface species. The substrate area to ECA or THF volume ratio approximated that of a 100 µm adhesive bond gap. The IP results mirrored 100 µm gap bond line polymerisation IPs that were observed in a recent related confocal Raman spectroscopy study of strong acid stabilised ECA curing on a range of substrates [12]. Initial results using thermistor-based measurements have shown that adsorption of cyanoacetic acid from a THF solution was also highly substrate dependent.

Migration of surface initiating species into bond line adhesive is thought to play an important role in CA curing. Limited experiments that used THF to extract surface nucleophiles confirmed this expectation for only some of the substrates that were tested. However, THF soluble nucleophiles did not measurably decrease the IPs of stabilised ECA in a 10 ppm MSA/THF test solution. Use of lower acid concentrations are required for a more sensitive measure of surface base solubility. The results show that surface adsorption could remove significant quantities of acid stabiliser and weak acid from bond line adhesive thereby greatly increasing the susceptibility of the adhesive to nucleophile initiated polymerisation. Use of low acid content monomer would give a more representative picture of stabilising acid interactions in CA bond line curing. In a wider context, the calorimetry techniques could be used for measurement of the acid /base contents of CA compatible solvents combinations.

7. Competing Interests

The authors declare that they have no competing interests.

8. Acknowledgement

The FOCAS Institute is funded under the National Development Plan 2000-2006 with assistance from the European Regional Development Fund. The authors gratefully acknowledge the award of a TU Dublin-Henkel Enterprise Scholarship for the support and supply of many materials.

References

[1] D.S. Johnston, D.C. Pepper, Polymerisation via macrozwitterions, 1. Ethyl and butyl cyanoacrylates polymerised by triethyl and triphenylphosphines, Die Makromolekulare Chemie. 182 (1981) 393–406. https://doi.org/10.1002/macp.1981.021820213.

[2] G.Costa, J.P.Cronin, D.C. Pepper, Termination and Transfer by acids in the Pyridine-Initiatied Polymerisation of Butyl Cyanoacrylate, European Polymer Journal. 19 (1983) 939–945. https://doi.org/10.1016/0014-3057(83)90053-8.

[3] G. Costa, C. Loonan, D. Pepper, End-group evidence of zwitterionic species in the anionic polymerization of cyanoacrylates by Lewis bases, Macromolecular Rapid Communications. 18 (1997) 891–896. https://doi.org/10.1002/marc.1997.030180918.

[4] E.F. Donnelly, D.S. Johnston, D.C. Pepper., Ionic and Zwitterionic Polymerization of n-Alkyl 2-Cyanoacrylate, Polymer Letter Edition. 15 (1977) 399–405. https://doi.org/10.1002/pol.1977.130150703.

[5] D.C. Pepper, The kinetics of slow-initiated living polymerizations, European Polymer Journal. 16 (1980) 407–411. https://doi.org/10.1016/0014-3057(80)90146-9.

[6] D.C. Pepper, Transfer by weak acids in the slow initiation-no-termination (SINT) polymerization of butyl cyanoacrylate, Makromol. Chem. 188 (1987) 527–536. https://doi.org/10.1002/macp.1987.021880307.

[7] D.C. Pepper, B. Ryan, Initiation Processes in Polymerizations of Alkyl Cyanoacrylates by Tertiary Amines: Inhibition by Strong Acids, Makromolekulare Chemie. 184 (1983) 383–394. https://doi.org/10.1002/macp.1983.021840214.

[8] D.C. Pepper, B. Ryan, Kinetics of Polymerization of Alkyl Cyanoacrylates by Tertiary Amines and Phosphines, Makromolecular Chemistry. 184 (1983) 395–410. https://doi.org/10.1002/macp.1983.021840215.

[9] I. Clement, D.C. Pepper, Propagation rate constants, Die Makromolekulare Chemie. 190 (1989) 3095–3103. https://doi.org/https://doi.org/10.1002/macp.1989.021901207.

[10] T.A. Bykova, Y.G. Kiparisova, B. v. Lebedev, K.A. Mager, Y.G. Gololobov, A calorimetric study of ethyl-α-cyanoacrylate and its polymerization and a study of polyethyl-α-cyanoacrylate at 13-450 K and normal pressure, Polymer Science U.S.S.R. 33 (1991) 537–543. https://doi.org/10.1016/0032-3950(91)90255-O.

[11] T. Stefanov, B. Ryan, A. Ivanković, N. Murphy, Mechanical bulk properties and fracture toughness of composite-to-composite joints of an elastomer-toughened ethyl cyanoacrylate adhesive, International Journal of Adhesion and Adhesives. 68 (2016) 142–155. https://doi.org/10.1016/j.ijadhadh.2016.03.001.

[12] K. Raheem, J. Cassidy, A. Betts, B. Ryan, Use of confocal Raman microscopy to characterise ethyl cyanoacrylate adhesive depth curing, Physical Chemistry Chemical Physics. 22 (2020). https://doi.org/10.1039/D0CP04053C.

[13] H. Hattori, Solid base catalysts: Generation of basic sites and application to organic synthesis, Applied Catalysis A: General. 222 (2001) 247–259. https://doi.org/10.1016/S0926-860X(01)00839-0.

[14] H.A. Benesi, B.H.C. Winquist, Surface Acidity of Solid Catalysts, Advances in Catalysis. 27 (1979) 97–182. https://doi.org/10.1016/S0360-0564(08)60055-3.

[15] A. Zheng, S. bin Liu, F. Deng, Acidity characterization of heterogeneous catalysts by solid-state NMR spectroscopy using probe molecules, Solid State Nuclear Magnetic Resonance. 55–56 (2013) 12–27. https://doi.org/10.1016/j.ssnmr.2013.09.001.

[16] J. W. Ntalikwa, Determination of surface charge density of α-alumina by Acid - base titration, Bulletin of the Chemical Society of Ethiopia. 21 (2007) 117–128. https://doi.org/10.4314/bcse.v21i1.61391.

[17] E. Tombácz, Ph-dependent surface charging of metal oxides, Periodica Polytechnica Chemical Engineering. 53 (2009) 77–86. https://doi.org/10.3311/pp.ch.2009-2.08.

[18] A. Auroux, Acidity and basicity: Determination by adsorption microcalorimetry, Molecular Sieves - Science and Technology. 6 (2008) 45–152. https://doi.org/10.1007/3829_008.

[19] A. Gervasini, A. Auroux, Microcalorimetric investigation of the acidity and basicity of metal oxides, Journal of Thermal Analysis. 37 (1991) 1737–1744. https://doi.org/10.1007/BF01912203.

[20] Aline. Auroux, Antonella. Gervasini, Microcalorimetric study of the acidity and basicity of metal oxide surfaces, The Journal of Physical Chemistry. 94 (1990) 6371–6379. https://doi.org/10.1021/j100379a041.

[21] V. Solinas, I. Ferino, Microcalorimetric characterisation of acid-basic catalysts, 1998. https://doi.org/10.1016/S0920-5861(98)00048-0.

[22] X. Chen, D. Huang, L. He, L. Zhang, Y. Ren, X. Chen, B. Yue, H. He, Effect of adsorbed water molecules on the surface acidity of niobium and tantalum oxides studied by mas nmr, Journal of Physical Chemistry C. 125 (2021) 9330–9341. https://doi.org/10.1021/acs.jpcc.1c02230.

[23] J. Granados-Reyes, P. Salagre, Y. Cesteros, G. Busca, E. Finocchio, Assessment through FT-IR of surface acidity and basicity of hydrocalumites by nitrile adsorption, Applied Clay Science. 180 (2019) 105180. https://doi.org/10.1016/j.clay.2019.105180.

[24] K. Coenen, F. Gallucci, B. Mezari, E. Hensen, M. van Sint Annaland, An in-situ IR study on the adsorption of CO2 and H2O on hydrotalcites, Journal of CO2 Utilization. 24 (2018) 228–239. https://doi.org/10.1016/j.jcou.2018.01.008.

[25] T.L. Silbaugh, J.S. Boaventura, M.A. Barteau, Surface acidity scales: Experimental measurements of Brønsted acidities on anatase TiO2 and comparison with coinage metal surfaces, Surface Science. 650 (2016) 64–70. https://doi.org/10.1016/j.susc.2015.11.022.

[26] G. Busca, The surface acidity of solid oxides and its characterization by IR spectroscopic methods. An attempt at systematization, Physical Chemistry Chemical Physics. 1 (1999) 723–736. https://doi.org/10.1039/a808366e.

[27] W. Rudziński, R. Charmas, T. Borowiecki, On the nature of the energetic heterogeneity of water/oxide interface in adsorption phenomena occurring at oxide surfaces, in: B.A. Averill (Ed.), Studies in Surface Science and Catalysis, 179th ed., Elsevier Science, Amsterdam, 1996: pp. 357–409. https://doi.org/10.1016/S0167-2991(06)81028-1.

[28] G. Rubasinghege, V.H. Grassian, Role(s) of adsorbed water in the surface chemistry of environmental interfaces, Chemical Communications. 49 (2013) 3071–3094. https://doi.org/10.1039/c3cc38872g.

[29] P.C. Stair, The Concept of Lewis Acids and Bases Applied to Surfaces, Journal of the American Chemical Society. 104 (1982) 4044–4052. https://doi.org/10.1021/ja00379a002.

[30] H. Chen, C.O. Stanier, M.A. Young, V.H. Grassian, A Kinetic Study of Ozone Decomposition on Illuminated Oxide Surfaces, The Journal of Physical Chemistry A. 115 (2011) 11979–11987. https://doi.org/10.1021/jp208164v.

[31] V.M. Muggeo, Segmented: An R package to Fit Regression Models with Broken-Line Relationships, R News. 8 (2008) 20–25. https://doi.org/10.1159/000323281.

[32] V.M.R. Muggeo, Interval estimation for the breakpoint in segmented regression: a smoothed score-based approach, Australian and New Zealand Journal of Statistics. 59 (2017) 311–322. https://doi.org/10.1111/anzs.12200.

[33] V.M.R. Muggeo, Estimating regression models with unknown break-points., Statistics in Medicine. 22 (2003) 3055–71. https://doi.org/10.1002/sim.1545.

[34] B.C. Bunker, Molecular mechanisms for corrosion of silica and silicate glasses, Journal of Non-Crystalline Solids. 179 (1994) 300–308. https://doi.org/10.1016/0022-3093(94)90708-0.

[35] I. Pignatelli, A. Kumar, M. Bauchy, G. Sant, Topological control on silicates' dissolution kinetics, Langmuir. 32 (2016) 4434–4439. https://doi.org/10.1021/acs.langmuir.6b00359.

[36] P.N.H. Nakashima, The Crystallography of Aluminum and Its Alloys, in: Encyclopedia of Aluminum and Its Alloys, CRC Press, Boca Raton, 2019. https://doi.org/10.1201/9781351045636-140000245.

[37] M. Bauccio, ASM Metals Reference Book, Third Edit, ASM International, Ohio, 1993.

[38] D.W. Smith, An acidity scale for binary oxides, Journal of Chemical Education. 64 (1987) 480. https://doi.org/10.1021/ed064p480.

[39] E. McCafferty, Lewis Acid/Lewis Base Effects in Corrosion and Polymer Adhesion at Aluminum Surfaces, Journal of The Electrochemical Society. 150 (2003) B342. https://doi.org/10.1149/1.1580135.

[40] H. Li, C. Dong, K. Xiao, X. Li, P. Zhong, Effect of alloying elements on the corrosion behavior of 0Cr12Ni3Co12Mo4W ultra high strength stainless steel, International Journal of Electrochemical Science. 10 (2015) 10173–10187.

[41] Y. Fang, M. Tang, V.H. Grassian, Competition between Displacement and Dissociation of a Strong Acid Compared to a Weak Acid Adsorbed on Silica Particle Surfaces: The Role of Adsorbed Water, Journal of Physical Chemistry A. 120 (2016) 4016–4024. https://doi.org/10.1021/acs.jpca.6b02262.

[42] A.L. Goodman, E.T. Bernard, V.H. Grassian, Spectroscopic Study of Nitric Acid and Water Adsorption on Oxide Particles: Enhanced Nitric Acid Uptake Kinetics in the Presence of Adsorbed Water, The Journal of Physical Chemistry A. 105 (2001) 6443–6457. https://doi.org/10.1021/jp003722l.

[43] I. C. Eromosele, D. C. Pepper, B Ryan, Water effects on the zwitterionic polymerization of cyanoacrylates, Makromol. Chem. 190, 1613 - 1622 (1989)